# Describing static correlation in bond dissociation by Kohn-Sham density functional theory

M. Fuchs,[1,2] Y.-M. Niquet,[2,3] X. Gonze,[2] and K. Burke[4]

[1] *Fritz-Haber-Institut der Max-Planck-Gesellschaft, Faradayweg 4-6, D-14195 Berlin, Germany*
[2] *Unité PCPM, Université Catholique de Louvain, 1348 Louvain-la-Neuve, Belgium*
[3] *Département de Recherche Fondamentale sur la Matière Condensée, SP2M/L_Sim, CEA Grenoble, 38054 Grenoble Cedex 9, France*
[4] *Dept. of Chemistry and Chemical Biology, Rutgers University, 610 Taylor Road, Piscataway, NJ 08854*

(Dated: February 2, 2008)

We show that density functional theory within the RPA (random phase approximation for the exchange-correlation energy) provides a correct description of bond dissociation in $H_2$ in a spin-restricted Kohn-Sham formalism, i.e. without artificial symmetry breaking. We present accurate adiabatic connection curves both at equilibrium and beyond the Coulson-Fisher point. The strong curvature at large bond length implies important static (left-right) correlation, justifying modern hybrid functional constructions but also demonstrating their limitations. Although exact at infinite and accurate around the equilibrium bond length, the RPA dissociation curve displays unphysical repulsion at larger but finite bond lengths. Going beyond the RPA by including the exact exchange kernel (RPA+X), we find a similar repulsion. We argue that this deficiency is due to the absence of double excitations in adiabatic linear response theory. Further analyzing the $H_2$ dissociation limit we show that the RPA+X is not size-consistent, in contrast to the RPA.

PACS numbers: 31.15.Ew, 31.25.Eb, 31.25.Nj

## I. INTRODUCTION

Density functional theory [1–3] (DFT) has proved to be a powerful method for calculating (and analyzing) the ground-state properties of molecular and condensed matter. In its standard Kohn-Sham (KS) form, the density $n(\mathbf{r})$ and total energy are constructed from the self-consistent solution of one-electron equations where, in practice, the exchange-correlation (XC) energy functional $E_{\rm XC}[n]$ must be approximated. Already the simple local-density approximation (LDA) and, more so, generalized gradient approximations (GGAs) can yield a remarkably realistic description of chemical bonds in solid and molecular systems. The state of the art is presently set by hybrid functionals [4, 5] that admix a fraction of the exact (Fock) exchange energy with GGA exchange. Achieving on the average nearly chemical accuracy for bond dissociation energies, they rival much more demanding post-Hartree-Fock configuration interaction or coupled cluster methods.

However there remain well-known conceptual limitations, with a clear practical significance, as exemplified by the following paradigm situations. (*i*) Long-ranged Coulomb correlations between non overlapping systems are not included in local functionals such as the LDA or GGAs (and thus also hybrids) but require fully nonlocal XC energy functionals [6–8]. Indeed LDA and GGAs perform at best erratically for van der Waals bonded systems [9, 10]. (*ii*) Scaling to the high-density or weakly-interacting regime, hybrid functionals do not properly recover the exact KS exchange energy [11]. This failure prominently concerns odd electron bonds, as exemplified by the $H_2^+$ molecule, where 100% exact exchange mixing and zero correlation energy would be needed [12, 13]. (*iii*) In systems with significant static (non-dynamical) correlation, LDA, GGA, and thus hybrid functionals underestimate the magnitude of the correlation energy [14, 15]. This becomes particularly problematic for the dissociation of electron pair bonds where near degeneracy effects arise in the molecular wavefunction. A famous example is the dissociating $H_2$ molecule: the proper (singlet) KS ground state at larger bond lengths has much too high total energy for such functionals. Usually one works around the problem: performing a spin-unrestricted calculation, a second solution with reasonable, lower energy is obtained. This succeeds because exchange functionals can mimic the static (i.e. long-ranged left-right) correlation and thus compensate for an error of the LDA and GGA type correlation functionals that describe effectively only dynamical correlation coming from electron repulsion at short range [15]. Yet the spin-unrestricted KS molecular wavefunction artifically breaks the symmetry of the dissociating molecule, displaying unphysical non-zero spin-polarization [16]. In fact *spurious* symmetry breaking has remained a much discussed drawback of spin-unrestricted DFT (and Hartree-Fock) calculations of molecular properties (see e.g. Refs. [17–20]).

Progress in each of the above noted respects may be achieved through orbital-dependent XC functionals expressed in terms of the (occupied and unoccupied) KS eigenstates, such as the Random Phase Approximation (RPA). The RPA functional is the simplest realization of the adiabatic-connection fluctuation-dissipation formalism [21] that defines a broad class of fully nonlocal XC functionals. In terms of the "Jacob's ladder" of density functional approximations [22], RPA is on the top rung, putting it among the most general (but also the

most demanding) of present-day approximations. It includes the exact KS exchange energy [23] as well as long-ranged Coulomb correlations giving rise to dispersion forces [6, 24]. This makes the RPA a natural starting point to address the above limitations $(i)-(iii)$ of existing functionals in a seamless and consistent way. In this paper we show that RPA functional is able to describe the strong static correlation in the dissociation of the $H_2$ bond in a *spin-restricted* KS formalism, without artificial symmetry breaking. The transition from mostly dynamical to strong static correlation is discussed in terms of the adiabatic connection. Analyzing the dissociation energy curve of $H_2$, we find that the RPA is accurate around the equilibrium bond length and yields, asymptotically, the correct dissociation into two H atoms. At intermediate distances the dissociation energy still displays an erroneous repulsion. Of course the RPA is just the first step in an ongoing systematic quest, with encouraging results for small molecules [25, 26] as well as van der Waals bonded structures [24, 27, 28]. To achieve satisfactory accuracy globally it requires extensions, some of which are being examined already [8, 23, 26, 29–31].

Last we would like to mention that the XC energy can be approximated also as functional of the one-electron density matrix, by making an appropriate ansatz for the exchange and correlation hole functions. For a particular such functional involving both the occupied and the unoccupied KS states, Grüning *et al.* [32] recently reproduced the entire dissociation energy curve of $H_2$, including proper dissociation. The validity of this approach is however still under debate [33].

Our paper is organized as follows. In Sec. II we first recall the classic problem of stretched $H_2$ and its implications in the context of different density functionals, and briefly discuss ways of dealing with it. We also summarize the RPA equations. In Sec. III we examine the XC energy of $H_2$ in the framework of the adiabatic connection, then, in Sec. IV we present and discuss our results for the RPA dissociation energy curve for $H_2$, and comment on current limitations and ways to overcome them. The Sec. V is devoted to results obtained beyond the RPA. Section VI summarizes our conclusions.

## II. THE PROBLEM OF STRETCHED $H_2$ IN DFT

A long-standing problem confronting all single-determinant calculations is that of stretched $H_2$, representative for the dissociation of electron pair bonds in general [3, 16, 34]. For *any* bond length $R$ the true (interacting) ground state is a singlet [35], with equal spin-up and spin-down densities, and the true (noninteracting) KS ground-state corresponds to a single Slater determinant $\Psi^{\rm KS} = |\sigma_g\overline{\sigma}_g|$ made up from the bonding $\sigma_g$ molecular orbital. The spin-restricted LDA, GGA, and hybrid functionals (as well as Hartree-Fock) correctly yield such a ground state, with reasonable total energy, around the equilibrium bond length $R_0$. As a matter of fact, the interacting ground state is also mainly of $|\sigma_g\overline{\sigma}_g|$ nature around $R \approx R_0$. However, as the bond length $R$ is increased toward $R \to \infty$, $\Psi^{\rm KS}$ no longer resembles the interacting ground state wavefunction of the molecule. Asymptotically the latter assumes the familiar Heitler-London form and puts precisely one electron on each of the two hydrogen atoms, completely suppressing number fluctuations and describing two free hydrogen atoms, i.e. $H^{\cdot}\cdots H^{\cdot}$ [16]. By contrast $\Psi^{\rm KS}$ is half contaminated by ionic contributions of the form $|s_a\overline{s}_a|$ and $|s_b\overline{s}_b|$ ($s_a$ and $s_b$ stand for the $1s$ orbitals centered on hydrogen A and B respectively), in effect describing the stretched $H_2$ as $\frac{1}{2}(H^{\cdot}\cdots H^{\cdot}) + \frac{1}{2}(H^{+}\cdots H^{-})$ [36]. Optimizing e.g. within spin-restricted GGA, the $\sigma_g$ orbital does not become a linear combination of the $1s$ hydrogenic orbitals but gets much too diffuse, in order to avoid the $H^-$ contribution. Hence the dissociation energy of stretched $H_2$ is severely overestimated, its total energy lying much above the one of two free hydrogen atoms (as illustrated later by our Fig. 5). On the other hand, a second solution with *lower* (and reasonable) energy may be obtained for bond lengths beyond the so-called Coulson-Fisher point [37, 38] by breaking the spin-symmetry and localizing on one hydrogen atom the "spin-up" electron and on the other the "spin-down" electron. This is what is obtained, in practice, by performing spin-unrestricted L(S)DA, GGA, or hybrid functional (as well as unrestricted Hartree-Fock) calculations.

This situation for approximate XC functionals embodies the well-known spin symmetry dilemma for dissociating $H_2$: restricted KS schemes yield the proper symmetry adapted ground-state but poor total energies, while unrestricted KS schemes yield very reasonable total energies but qualitatively wrong spin densities [16].

### A. Local, semilocal, and hybrid functionals

A discussion of this dilemma might appear academic, since in most cases one simply calculates the chemically bonded system, and subtracts from it the energies of the isolated atoms, without ever watching the molecule dissociate. However, at the origin of the problem is the inability of present XC functionals to properly capture long ranged left-right correlation that eventually appears when a molecule dissociates [39]. Such static (or non-dynamical) correlation is present in many real molecules even in or near the ground-state geometry. As a matter of fact LDA and GGA calculations only mimic it through their exchange component while their correlation component accounts for (short-ranged) dynamical correlation only (see e.g. Ref. [15]). In fact their performance depends crucially on the well-known cancellation of errors between exchange and correlation [11]. This compensation is of course neither perfect nor universal, as indicated by the on average overestimated atomization energies, particularly for multiply-bonded species like $N_2$,

but also by often underestimated reaction energy barriers (see e.g. Ref. [40]).

Hybrid functionals [4, 5] can provide a useful remedy and are usually more accurate than LDA or GGAs alone. Yet they still rely on a similar philosophy: the admixing of a certain *fixed* fraction of the (possibly spin-unrestricted) exact exchange energy can be understood to improve the description of static correlation while dynamical correlation is still described by (semi-) local LDA or GGA functionals. The errors in the exchange and correlation energies do not sufficiently cancel in cases where either exchange (paradigm: $H_2^+$) or static correlation (paradigm: dissociated $H_2$) prevail, so that eventually hybrid functionals can become inadequate too [14]. For dissociating electron pair bonds, sufficiently negative exchange energies are obtained only by resorting to spin-unrestricted exchange, i.e. by an unphysical breaking of the symmetry of the KS molecular wavefunction. At which bond length the spin-unrestricted solution becomes energetically preferable depends on the functional. Hybrid functionals are more prone to break symmetry with an increased admixing of exact exchange (see Ref. [41]). Artificially symmetry broken solutions from spin-unrestricted methods may also yield unphysical molecular properties, despite providing a lower energy solution and appearing better variationally [18]. We return to the concept of hybrid functionals in Sec. III A.

### B. Functionals of occupied and unoccupied KS states

Although the physical origin of the above difficulties is clear it is far from simple to correct for them, while retaining low computational cost. A variety of approaches have been applied, mostly along the same lines as a traditional restricted Hartree-Fock calculation would be corrected, such as spin-unrestricted [38], multi-reference [42, 43], or ensemble-referenced Kohn-Sham schemes [19, 44]. Although often useful, these suffer from similar difficulties as in Hartree-Fock, namely that different approaches work for different situations.

A more satisfying approach is to develop a more demanding but non-empirical scheme. Functionals involving occupied and unoccupied (virtual) KS orbitals offer this possibility as recently shown by Baerends and coworkers [32, 34]. A well-defined starting point is the exact exchange formalism (EXX) in Kohn-Sham DFT [45] which then must be complemented with a compatible correlation functional, i.e., one that properly respects the weakly-correlated, exchange-only limit (e.g. producing zero correlation energy in one-electron systems such as $H_2^+$) and accurately interpolates to the strongly-coupled regime to be discussed in Sec. III A. The RPA XC functional, discussed next in Sec. II C represents a possible first step into this direction.

### C. Functionals from linear response: RPA and beyond

The combination of the random-phase approximation (RPA) with DFT was discussed as early as the late 70's [21], then for the uniform electron gas. The idea is to start from the non-interacting KS response function and dress it with a (scaled) Coulomb interaction $\lambda\hat{v}_{\rm ee}$, and eventually also with an exchange-correlation kernel of time-dependent DFT (TDDFT) [46]. This yields the response function of an interacting system, which by way of the fluctuation-dissipation theorem gives the corresponding pair-correlation function and thus the electron-electron interaction energy. The XC energy is last obtained through an integration of the electron-electron interaction energy along an adiabatic path connecting the non-interacting KS system ($\lambda = 0$) to the interacting one ($\lambda = 1$, see Sec. III A).

Working in the imaginary frequency ($iu$) domain, the basic equations (in Hartree atomic units) are as follows. Starting from a KS ground-state with eigenstates $\{\phi_{i\sigma}[n], \epsilon_{i\sigma}[n]\}$, functionals of the density $n$, one constructs the KS response

$$\chi^0(\mathbf{r},\mathbf{r}';iu) = \sum_{\sigma,k,l} \frac{(\gamma_{k\sigma}-\gamma_{l\sigma})}{iu-(\varepsilon_{l\sigma}-\varepsilon_{k\sigma})} \times\phi^*_{k\sigma}(\mathbf{r})\phi_{l\sigma}(\mathbf{r})\phi^*_{l\sigma}(\mathbf{r}')\phi_{k\sigma}(\mathbf{r}') \quad , \quad (1)$$

with $\gamma_{i\sigma} = 1$ for occupied and $\gamma_{i\sigma} = 0$ for unoccupied KS states. The interacting response function $\chi^\lambda$ at coupling strength $\lambda$ follows from the Dyson-type screening equation

$$\chi^\lambda(iu) = \chi^0(iu)[1-\left(\lambda v_{\rm ee} + f^\lambda_{\rm XC}(iu)\right)\chi^0(iu)]^{-1} \quad , \quad (2)$$

where $v_{\rm ee} = 1/|\mathbf{r}-\mathbf{r}'|$ is the Coulomb repulsion and $f^\lambda_{\rm XC}(iu)$ stands for the XC kernel of TDDFT (matrix notation $A =: A(\mathbf{r},\mathbf{r}')$ and $AB =: \int d^3r'' A(\mathbf{r},\mathbf{r}'')B(\mathbf{r}'',\mathbf{r}')$ is implied here). The fluctuation-dissipation theorem and the coupling strength integration (see Sec. III A) finally yield an exact expression for the XC energy:

$$E_{\rm XC}[n] = -\frac{1}{2}\int_0^1 d\lambda \int d^3r d^3r' \frac{1}{|\mathbf{r}-\mathbf{r}'|} \times\left[\left\{\int_0^\infty \frac{du}{\pi}\,\chi^\lambda(\mathbf{r},\mathbf{r}';iu)\right\} + n(\mathbf{r})\delta(\mathbf{r}-\mathbf{r}')\right] \quad (3)$$

called the adiabatic-connection fluctuation-dissipation theorem (ACFDT) for the XC energy. Through approximations for $f^\lambda_{\rm XC}$, fully nonlocal ACFDT XC functionals can be generated in practice. In general these will be orbital-dependent functionals involving, through $\chi^0$ (and eventually $f^\lambda_{\rm XC}$), both occupied and unoccupied KS states. The RPA is obtained by setting $f^\lambda_{\rm XC} = 0$, i.e. neglecting all XC contributions to screening in Eq. 2. Approximating $f^\lambda_{\rm XC}$ by the (exact) exchange kernel of TDDFT [46] defines the RPA+X functional. In the ACFDT formula (Eq. 3), because of the integral over

the coupling strength, an approximation to $\chi^\lambda$ of a given order in $\lambda$, produces an approximation to $E_{\rm XC}[n]$ to the next highest order. Thus, to zeroth order, $\chi^0$ inserted in Eq. 3 yields the exact exchange energy, $E_{\rm X}[n]$, the first-order energy. The RPA yields an approximation to $E_{\rm XC}$ that contains all orders of $\lambda$, but misses contributions from second-order onward. In RPA+X on the other hand $f_{\rm XC}^\lambda$ (and thus $\chi^\lambda$) are treated exactly up to first-order. In turn the RPA+X yields an approximation to $E_{\rm XC}[n]$ that is exact up to second-order but, in an approximate way, again includes also all high orders of $\lambda$. Being exact to second-order, the RPA+X produces the exact initial slope of the adiabatic connection (to be discussed in detail in Sec. III A) as given by second-order Görling-Levy perturbation theory (GL2) [47].

While the RPA is expected to be quite accurate for (iso-electronic) total energy differences, it tends to underestimate absolute correlation energies [23]. Indeed, the short-range behavior of $\chi^{\rm RPA}$ is incorrect, because the electrons only respond to the averaged density fluctuations. In particular, the (spurious) "self-response" of an electron to its own contribution to these density fluctuations is the most important source of error in few electron systems. It is responsible for a (spurious) non-zero self-correlation energy in one-electron systems like the H atom. This deficiency of the RPA may well be corrected by a local-density functional $E_{\rm C}^{\rm sr-LDA}[n]$ designed for the purpose [23], defining the so-called "RPA+" functional $E_{\rm XC}^{\rm RPA+}[n] = E_{\rm XC}^{\rm RPA}[n] + E_{\rm C}^{\rm sr-LDA}[n]$. As expected in Refs. [23, 29] and confirmed in Refs. [25, 26], local or semilocal short-ranged corrections have rather minor effects on molecular dissociation energies, yet nicely correct for spurious RPA self-response problem in the H and He atoms [26]. For these reasons we focus in this paper on the *difference* of the total energies and XC energies between the molecule and the isolated atoms.

Compared to likewise orbital-dependent Meta-GGAs [48–50] and hybrid functionals, the RPA involves both *occupied* and *unoccupied* KS states. Its computational cost is quite severe (a factor $10^2 \ldots 10^3$ compared to a GGA approach), but its promise is to tackle the nonlocality of exchange and correlation on an equal footing, leading to a seamless description from the chemically-bonded to the dissociated regime, including van der Waals interactions not accounted for in GGAs or hybrids.

Recent calculations for small molecules by Furche [25] found that the RPA describes the chemical bonds with similar but not better accuracy as modern GGAs. Although this appears to be disappointing, we note that the RPA is in fact accurate for $H_2$ and the difficult case of $Be_2$ [26] where LDA and GGA fail. Also there has been significant progress in building XC functionals on top of the RPA that include the dispersion forces between layered solid-state structures such as jellium slab models [24] and graphite [27], and between atoms or molecules [28]. We further point out that the RPA is just a ready realization of a much broader class of functionals based on the adiabatic-connection fluctuation-dissipation theorem which offers various options for improvements [26, 29–31]. Moreover the RPA is amenable to extensions derived in many-body Green function theory which itself is being very actively explored for total energy calculations [10, 51, 52], including $H_2$ [53–55].

In the present study we do not perform self-consistent RPA calculations, these are computationally too costly at present (although formally perfectly feasible, see Refs. [56, 57]). Instead we evaluate Eqs. 1 - 3 *a posteriori* with the KS eigenstates taken from EXX calculations as explained further in Sec. III D. Thanks to the variational principle for DFT total energies we expect the resulting RPA total energies to be tight upper bounds to the self-consistent RPA results. Indeed we found that our results for the RPA total energies remained virtually unchanged when we used the LDA [58] or PBE GGA [59] instead of the EXX for calculating the initial KS states.

## III. ANALYSIS OF THE $H_2$ DISSOCIATION

In this section and in the next one, we show that the RPA offers a promising handle on the problem of dissociating electron pair bonds as exemplified by $H_2$. In particular, we give the correct prescription for applying the scheme during dissociation and show that its remaining errors may well be correctable. Using it, we also provide the first accurate calculations of adiabatic connection curves as a system passes through its Coulson-Fisher point where the KS ground-state for standard XC functionals bifurcates in a spin-symmetry adapted and a lower energy but symmetry-broken solution.

### A. Adiabatic connection

To understand in detail how DFT handles static correlation, one invokes the adiabatic connection [21, 38], already briefly mentioned in Sec. II C. One imagines altering the strength of the electron-electron repulsion by multiplying it by a constant $\lambda$, which varies between 0 and 1. At the same time, the one-body potential is altered, i.e., made a function of $\lambda$, so as to keep the electron density fixed. This is a way of continuously connecting the noninteracting KS system ($\lambda = 0$) to the interacting physical system ($\lambda = 1$). More importantly, by virtue of the Hellmann-Feynman theorem, one can write the XC energy as an integral over purely potential energy:

$$E_{\rm XC}[n] = \int_0^1 d\lambda \; U_{\rm XC}[n](\lambda) \tag{4}$$

where $U_{\rm XC}[n](\lambda) = \langle \Psi^\lambda[n] | \hat{v}_{\rm ee} | \Psi^\lambda[n] \rangle - U[n]$. Here $\Psi^\lambda[n]$ is the ground-state wavefunction at coupling strength $\lambda$, $\hat{v}_{\rm ee}$ is the Coulomb repulsion, and $U[n]$ is the Hartree energy. The integrand $U_{\rm XC}[n](\lambda)$ represents the potential energy contribution to XC and makes up the adiabatic

connection curve. At the $\lambda = 0$ end it corresponds to the exact Kohn-Sham exchange energy $E_{\rm x}$ [23],

$$U_{\rm xc}[n](0) = E_{\rm x}[n] \quad , \tag{5}$$

and has a (negative) initial slope, given by the correlation energy of second-order Görling-Levy perturbation theory (GL2) [47]

$$U'_{\rm xc}[n](\lambda) = \frac{d}{d\lambda} U_{\rm xc}[n](\lambda)\Big|_{\lambda=0} = 2\, E_{\rm c}^{\rm GL2}[n] \quad . \tag{6}$$

All $\lambda$-dependence rests in the correlation contribution

$$U_{\rm c}[n](\lambda) = U_{\rm xc}[n](\lambda) - E_{\rm x}[n] \quad . \tag{7}$$

At $\lambda = 1$, $U_{\rm xc}[n](\lambda)$ describes the XC potential energy of the physical system, $U_{\rm xc}[n] =: U_{\rm xc}[n](1)$, and, similarly, the correlation potential energy, $U_{\rm c}[n] =: U_{\rm c}[n](1)$. Since correlation reduces the electron-electron repulsion, the different energies are always ordered as

$$E_{\rm x}[n] \geq E_{\rm xc}[n] \geq U_{\rm xc}[n] \quad . \tag{8}$$

The $\lambda$-dependence for ACFDT type functionals (see Eq. 3), appearing through the response function $\chi^\lambda$, is given by

$$U_{\rm c}[n](\lambda) = -\frac{1}{2}\int_0^\infty \frac{du}{\pi}\, {\rm Tr}\left[v_{\rm ee}\left\{\chi^\lambda(iu) - \chi^0(iu)\right\}\right] \quad , \tag{9}$$

where ${\rm Tr}[A] =: \int d^3r A(\mathbf{r},\mathbf{r})$. The full $\lambda$-curve may then be calculated thanks to Eq. 7. For the LDA or GGA type functionals the $\lambda$-dependence can be readily calculated from the exact relation [60]

$$U_{\rm xc}[n](\lambda) = \frac{d}{d\lambda}\left(\lambda^2 E_{\rm xc}[n_{1/\lambda}]\right) \quad , \tag{10}$$

where the XC energy functional is evaluated at the scaled density $n_{1/\lambda}(\mathbf{r}) =: n(\mathbf{r}/\lambda)/\lambda^3$. Hence analysis by adiabatic decomposition allows investigation into how well the different functionals perform, and why [11, 61].

Below we consider molecular dissociation energies, i.e. the difference between the molecular and atomic total energies,

$$\Delta E = E_{\rm tot}[\text{molecule}] - E_{\rm tot}[\text{atoms}] \quad , \tag{11}$$

and analyze the exchange-correlation contributions by means of the analogously defined differences $\Delta E_{\rm xc}$, $\Delta E_{\rm x}$, and $\Delta U_{\rm xc}(\lambda)$.

A useful measure of the correlation strength is given in Ref. [62]. Define the parameter $b$ by

$$E_{\rm xc}[n] = bE_{\rm x}[n] + (1-b)U_{\rm xc}[n] \quad . \tag{12}$$

A simple interpretation of $b$ is given by the following geometrical construction: if the adiabatic curve were a horizontal line of value $E_{\rm x}[n]$ running from 0 to $b$, and then dropped discontinuously to another horizontal line of value $U_{\rm xc}[n]$ running from $b$ to 1, then $b$ is that value of $\lambda$ that yields the correct $E_{\rm xc}[n]$. Thus, in the high density limit, where the adiabatic connection curve is a straight line, $b$ is exactly 1/2. On the other hand, for strong static correlation, in which the adiabatic connection curve drops rapidly to its final value, $b$ is close to zero. One can also show [62]

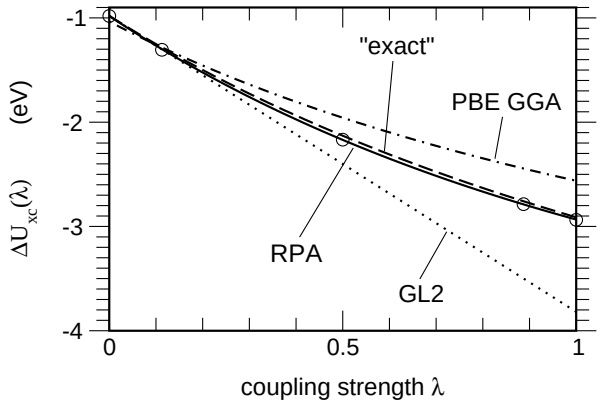


FIG. 1: Adiabatic connection for $H_2$ at bond length $R$ = 1.4 bohr within the RPA (solid line) and the GGA (dot-dashed line). The GL2 curve (dashed) corresponds to the slope of the exact curve at $\lambda = 0$. Shown is the difference between $H_2$ and two free H atoms, evaluated on self-consistent EXX densities. The "exact" curve is an interpolation [65] based on accurate values of $\Delta E_{\rm x}$, $\Delta E_{\rm xc}$, and $\Delta U_{\rm xc}$ from a configuration interaction calculation [63, 64].

$$b = \frac{T_{\rm c}[n]}{|U_{\rm c}[n]|} \quad , \tag{13}$$

where $T_{\rm c}$ is the kinetic portion of the correlation energy

$$T_{\rm c}[n] = E_{\rm c}[n] - U_{\rm c}[n] \quad . \tag{14}$$

Thus small $b$ indicates that the correlation is indeed static, i.e., has a smaller fraction of kinetic to potential energy.

For the atoms and most chemically bonded systems, the adiabatic connection curve is rather non-descript, lying close to a straight line. This is illustrated by $H_2$ at the equilibrium bond length in Fig. 1, where we plot $\Delta U_{\rm xc}^{\rm RPA}(\lambda)$. The area enclosed by the adiabatic connection curves represents the XC contribution to the dissociation energy, $\Delta E_{\rm xc}$. As can be seen from Tab. I the RPA dissociation energy of $H_2$ is excellent agreement with the exact value. Noting also the good agreement of the endpoints of our RPA curve in Fig. 1 with accurate data from configuration interaction calculations [63, 64], listed in Tab. I, this implies that the RPA curve lies very close to the true adiabatic connection curve. The straight line corresponds to GL2 theory, indicating the $b = 1/2$ high density limit and the initial slope of the true curve given by Eq. 6. For $\lambda > 0$, $\Delta U_{\rm xc}^{\rm GL2}(\lambda)$ lies below the true curve, overestimating the absolute correlation energy. Indeed, calculating $\chi^{\rm RPA+X}$ to first order in $\lambda$ we

TABLE I: Adiabatic decomposition of the dissociation energy $\Delta E$ of $H_2$ at bond length $R = 1.4$ bohr, evaluated on self-consistent EXX densities. Shown are the differences between the molecule and two free H atoms for the coupling strength integrand $\Delta U_{\rm XC}(\lambda)$ and related quantities, as explained in the text. All values are in eV.

| | $\Delta E$ | $\Delta E_{\rm XC}$ | $\Delta E_{\rm X}$ | $\Delta U_{\rm C}$ | $\frac{\Delta T_{\rm C}}{\lvert\Delta U_{\rm C}\rvert}$ | $\Delta U'_{\rm XC}(0)$ |
|---|---|---|---|---|---|---|
| PBE GGA | $-4.54$ | $-1.91$ | $-1.04$ | $-1.52$ | 0.431 | $-2.42$ |
| RPA | $-4.73$ | $-2.10$ | $-0.99$ | $-1.95$ | 0.427 | $-2.97$ |
| exact | $-4.74^a$ | $-2.04^b$ | $-0.98^b$ | $-1.93^b$ | 0.450 | $-2.84$ |

[a] Reference [35].

[b] From Refs. [63, 64]. In these works, $E_{\rm X}$, $E_{\rm XC}$, and $T_{\rm C}$ were calculated on the $H_2$ density obtained from a configuration interaction calculation which yielded $\Delta E = -4.68$ eV. Using these data we evaluated $\Delta U_{\rm C}$ from Eq. 14.

obtain $\Delta E^{\rm GL2} = -5.04$ eV, about 0.3 eV below the true dissociation energy. This indicates that the second-order perturbative treatment is qualitatively but not quantitatively accurate for $H_2$. Regarding the PBE GGA, Fig. 1 and Tab. I show that it is accurate for the exchange energy ($\lambda = 0$) but underestimates the absolute correlation potential energy ($\lambda = 1$). In turn the PBE GGA also underestimates the absolute XC energy and the dissociation energy of $H_2$.

Calculations of the exact adiabatic connection, using the accurate ground-state wavefunctions for all $\lambda$, have so far not been attempted to our knowledge for molecules, while a few such curves based on accurate ground-state densities have been reported for atoms [66–68], bulk Si [69], and model systems [70]. We remark that $\frac{d}{d\lambda}U_{\rm XC}[n](\lambda)|_{\lambda=0}$, i.e. the GL2 correlation energy, is also a key ingredient in a recent coupling strength interpolation of the adiabatic connection by Seidl *et al.* [71] which performs with similar accuracy as modern hybrid functionals for molecular dissociation energies. For $H_2$ close to the equilibrium bond length, the corresponding dissociation energy and adiabatic connection curve are in good agreement with our RPA results [72].

### B. $H_2$ symmetry dilemma

We now discuss the stretching of $H_2$ as a paradigm of the difficulties that single-determinant methods have with dissociation. The nearly straight line behavior dramatically changes when the bond is stretched to $R \to \infty$. Asymptotically, the proper molecular wavefunction for any $\lambda > 0$ (i.e. regardless of the interaction strength) is the bonding linear combination of the $1s$ orbitals of the two H atoms. For the $H_2$ "super-molecule" the exchange energy therefore has the same value as in a hydrogen atom, i.e. $E_{\rm X}[{\rm H}\cdot\cdots{\rm H}\cdot] \to E_{\rm X}[{\rm H}] = -U[n_{\rm H}]$. Consequently also $U_{\rm C}[{\rm H}\cdot\cdots{\rm H}\cdot](\lambda) \equiv -U[n_{\rm H}]$ for any $\lambda > 0$, since the dissociated $H_2$ molecule must have the same total energy as two H atoms. Figure 2 shows the corresponding exact adiabatic connection $\Delta U_{\rm XC}[{\rm H}\cdot\cdots{\rm H}\cdot](\lambda)$. The immediate drop of the adiabatic connection curve at $\lambda = 0$ is characteristic for a system with strong static correlation: here $b = 0$ exactly. The position of one electron entirely determines the position of the other electron: the two electrons in infinitely separated $H_2$ must sit on the two different nuclei but never on the same, as spuriously allowed by the single KS determinant. This type of correlation is often refered to as left-right or static correlation, where the true many-electron wavefunction takes on multi-determinant character [3]. Put differently [34], in the concept of the XC hole, the exchange hole of $H_2$ is spatially completely delocalized over both nuclei. However the XC true hole is always centered about the reference electron. This means that the correlation hole must be long-ranged to yield the proper hydrogen-like hole on one nucleus and the needed zero total XC hole on the opposite nucleus. By contrast LDA or GGA correlation holes, derived essentially from the uniform electron gas, are always short-ranged, and hence cannot cancel the exact exchange hole far away. Breaking inversion symmetry, L(S)DA and spin-dependent GGA on the other hand (like unrestricted Hartree-Fock) already yield the spin-up and -down exchange holes of separate hydrogen atoms, opposite spin electrons sitting on different nuclei, and thus mimic the static correlation: unrestricted Hartree-Fock or exact KS exchange indeed yield two hydrogen atoms as the dissociation products, and produce curves similar to Fig. 2.

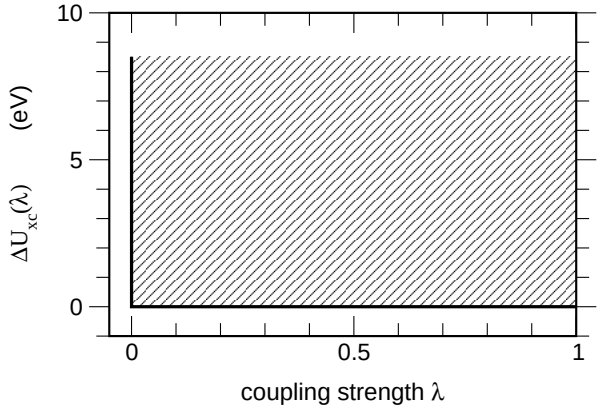


FIG. 2: Exact adiabatic connection for dissociated $H_2$ at bond length $R \to \infty$, shown as the difference with respect to two free H atoms. For the exact KS determinant the curve starts at $\lambda = 0$ with the negative of the exact exchange energy of a single H atom, $-E_{\rm X}({\rm H}) \simeq 8.5$ eV as explained in the text. The negative of the shaded area represents the correlation energy of the $H_2$ molecule and equals $E_{\rm X}({\rm H})$.

### C. Behavior of hybrid functionals

Does any of this matter for real systems, especially if we never ask them to dissociate? The answer is emphati-

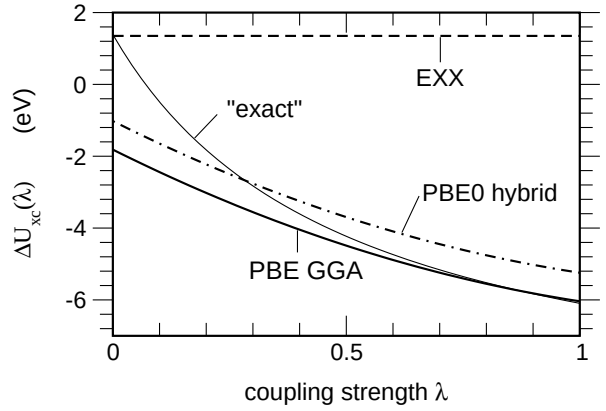


FIG. 3: Sketch of $\Delta U_{\rm XC}(\lambda)$ for $N_2 \rightarrow 2\,$N. (The EXX, PBE, and PBE0 hybrid curves are calculated from the self-consistent PBE densities and orbitals. The "exact" curve is an interpolation between $\Delta E_{\rm X}$ and $\Delta U_{\rm XC}^{\rm PBE}$, following Ref. [61].)

cally yes. Currently our most accurate popular functionals are hybrids, which mix a fraction $a_0 \approx 1/4$ of exact exchange with GGA. To understand why this improves the accuracy over GGAs [11], one first notes that usually the latter work best near $\lambda = 1$ ($H_2$ being an exception to this rule) [11]. But they worsen as $\lambda \to 0$, especially when there is static correlation in the system. The reason is twofold and illustrated in Fig. 3 for $N_2$ (where static correlation is expected to be most pronounced in the $\pi$ bonds). On the one hand GGA exchange energies tend to be too negative for molecules, leading to a too low starting point for the adiabatic connection at $\lambda = 0$. On the other hand the GGA correlation potential energy is accurate toward $\lambda = 1$, but too flat a function otherwise. As a consequence $\Delta U_{\rm XC}(\lambda)$ in the GGA lies too low, leading to an overestimate of the magnitude of the dissociation energy. Strong static correlation shows up as a rapid drop of $U_{\rm XC}(\lambda)$ from $\lambda = 0$ toward $\lambda = 1$. Note that the free N atoms contain little static correlation, that is, their $U_{\rm XC}(\lambda)$ lie close to a straight line and can be accurately obtained from GL2 perturbation theory. Recognizing that GGAs (and also the LDA) are typically least accurate at the $\lambda = 0$ end, hybrid functionals can improve over the GGA adiabatic connection by mixing in the exact exchange energy, i.e. part of the exact limit $U_{\rm XC}(0) = E_{\rm X}$. This has led to hybrid XC functionals of the generic form

$$E_{\rm XC}^{\rm hyb} = E_{\rm XC}^{\rm GGA} + a_0(E_{\rm X} - E_{\rm X}^{\rm GGA}) \quad . \qquad (15)$$

Becke has determined an emprirical value of $a_0 \approx 0.28$ [4]. The non-empirical estimate of $a_0 = 1/4$ has been given, based on the observation that $U_{\rm XC}(\lambda)$ is formally provided by DFT perturbation theory and fourth order is adequate for typical molecules, and defines the so-called PBE0 hybrid [5], shown for $N_2$ in Fig. 3. Hybrid functionals like the PBE0 on the average yield molecular dissociation energies close to chemical accuracy [73], improving over GGA. Pictorially, the admixing of exact exchange shifts the GGA curve a fraction $a_0$ toward the true starting point ($\lambda = 0$) of the correct curve. Since the true adiabatic connection curve drops sharply from $\lambda = 0$, a fraction $a_0 < 1/2$ produces a hybrid curve whose area is about that of the true curve, as in Fig. 3.

From the adiabatic connection we can also understand when (semi-)local and hybrid functionals become inappropriate. If the XC energy is dominated by exchange and there is little correlation energy, the adiabatic connection curve drops little from its $\lambda = 0$ value. For one-electron systems, such as in $H_2^+$, there is even zero correlation and the adiabatic connection curve stays completely flat. Then one ought to use $a_0 \approx 1$, i.e. 100% exact exchange. Indeed GGA as well as hybrid functionals perform poorly for one-electron bonds such as in radical ions [12, 13]. On the other hand if static correlation is important, the adiabatic connection will drop rapidly from its value at $\lambda = 0$, given by the exact exchange energy. This drop is missed by GGA correlation functionals, which then underestimate the correlation energy. This error may be compensated by using approximate GGA exchange functionals since these tend to overestimate the absolute exchange energy in molecules and the exchange contribution to dissociation energies [11]. Hybrids with $a_0 > 0$ improve the exchange energies over GGA alone but eventually also reduce the error cancellation due to GGA exchange. An early indication for this was the observation that combining 100% exact exchange with GGA correlation completely fails for molecular dissociation energies [74]. In fact no exact exchange mixing ($a_0 \approx 0$) can sometimes be the better choice as demonstrated in Ref. [14]. We stress that to describe strong static correlation effects in bond dissociation, any of these functionals must be used in spin-unrestricted form in order to attain exchange energies that are negative enough to compensate for the lack in the respective approximation for correlation. Clearly, to describe the transition from exchange dominated to static correlation dominated XC regimes, a more flexible, i.e. "system sensitive" interpolation of the adiabatic connection than provided by present hybrid functionals is needed [62].

### D. Beyond the Coulson-Fisher point

A key concept in this paper is that DFT within the RPA allows correct dissociation of molecules. However, given our present inability to perform self-consistent RPA calculations, the demonstration of this fact becomes quite subtle. While the (restricted) EXX solution is an adequate starting point for the RPA around the equilibrium bond length, it is totally inadequate beyond the Coulson-Fischer point ($R > 2.5$ bohr for $H_2$ treated in EXX), where ambiguity arises in a single-determinant calculation. In the words of the symmetry dilemma, should one use the unrestricted solution, which has a pretty good energy but totally incorrect spin density, or the restricted solution, which has the correct symmetry but poor ener-

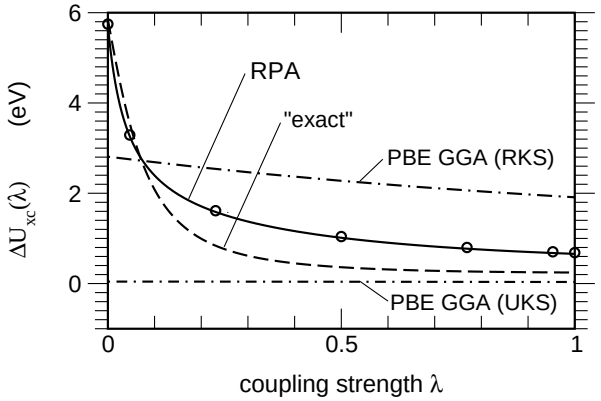


FIG. 4: Same as Fig. 1, but for $R = 5$ bohr, i.e. beyond the Coulson-Fisher point. The RPA results are based on the *total* density of a unrestricted EXX KS calculation. Also shown are the adiabatic connections for the PBE GGA applied in the restricted KS formalism (RKS), yielding poor energetics, and in the unrestricted KS formalism (UKS), yielding better energetics but artifically breaking inversion symmetry.

getics (as seen in Fig. 5) ?

The answer has been given in Ref. [16]. One must use the best estimate for the correct ground-state density that is available. As argued there, the unrestricted solution yields the best approximate DFT density, but its spin density is not to be believed. We therefore take the *total* density from our *unrestricted* EXX KS calculation, and treat it as a spin-singlet. This becomes our input density to our RPA calculation. Recall that this density becomes exact in the limit of $R \to \infty$, where it corresponds to two separate hydrogenic densities, in contrast to a *restricted* scheme. Inverting the KS equation [75] for $n(\mathbf{r}) = n_\uparrow^{\rm EXX}(\mathbf{r}) + n_\downarrow^{\rm EXX}(\mathbf{r})$, we obtain the KS potential yielding that density and the respective KS eigenstates.

## IV. $H_2$ DISSOCIATION WITHIN THE RPA

As can be seen from Fig. 4, the RPA adiabatic connection of $H_2$ beyond the Coulson-Fisher point becomes strongly bent downward, capturing the onsetting crucial contribution of static correlation related to the multideterminant nature of the interacting many-electron wave function. The latter is not captured in the PBE GGA correlation functional which significantly underestimates the magnitude of the correlation energy, as seen from Tab. II and evident from the PBE GGA (RKS) curve in Fig. 4. Switching to the *unrestricted* PBE (and PBE0) schemes, their exchange component simulates the missing static correlation while the correlation component is much too small in magnitude as Tab. II shows.

Correspondingly, *unrestricted* PBE (like PBE0) eventually give dissociation energies that are in quite good agreement with the exact value, as listed in Tab. III. We stress that this is a result of error cancellation between (unrestricted) exchange and correlation: the PBE adiabatic connection curves is qualitatively clearly wrong, especially at $\lambda = 0$, where its $\Delta E_{\rm x}$ is much too small and its slope turns out even slightly positive (though this is not visible on the scale of Fig. 4). No such error cancellation occurs within the RPA. The onset of strong static correlation is reflected in the low value of our correlation strength parameter $b$ reported in Tab. II for the RPA and exact curves, but not for (semi-) local density functional approximations.

Although qualitatively correct the RPA adiabatic connection curve is still deficient, as can be appreciated by comparing to the exact curve in Fig. 4 and data in Tab. II. $\Delta U_{\rm C}^{\rm RPA}(\lambda)$ does not drop deep enough with $\lambda$, despite its too steep initial slope. Correspondingly the RPA yields a too positive molecular correlation energy and produces an artificial barrier for dissociation as seen in Tab. III. This is further evidenced in the full RPA dissociation curve of Fig. 5. Indeed, while the RPA performs accurately around equilibrium $R$ and again at larger $R$, it shows an unphysical bump at intermediate bond length $R$. The origin of this bump will be further discussed below. Nonetheless the asymptotic behavior ($R \to \infty$) of the RPA is correct, as can be understood from a model

TABLE II: Adiabatic decomposition of the dissociation energy $\Delta E$ of $H_2$ at bond length $R = 5$ bohr, as shown in Fig. 4. The RPA functional is evaluated on the total density from a spin-unrestricted EXX calculation as described in Sec. III D. Also shown are results for the PBE GGA, evaluated as a spin-restricted (RKS) and a spin-unrestricted (UKS) functional using the EXX spin-densities. All values are in eV.

| | $\Delta E$ | $\Delta E_{\rm XC}$ | $\Delta E_{\rm X}$ | $\Delta U_{\rm C}$ | $\frac{\Delta T_{\rm C}}{\lvert\Delta U_{\rm C}\rvert}$ | $\Delta U'_{\rm XC}(0)$ |
|---|---|---|---|---|---|---|
| PBE (RKS) | 2.20 | 2.30 | 2.81 | −0.90 | 0.43 | −1.23 |
| PBE (UKS) | −0.06 | 0.040 | 0.044 | −0.008 | 0.50 | 0.084 |
| RPA | 0.54 | 1.33 | 5.72 | −5.06 | 0.13 | −111 |
| exact | −0.10[a] | 0.82[b] | 5.85[b] | −5.61[b] | 0.10 | −56.8 |

[a]Reference [35].
[b]From Refs. [63, 64], see also Tab. I.

TABLE III: Dissociation energy of $H_2$ at bond length $R$, calculated with different XC functionals as indicated in Fig. 5. Given are the energies from unrestricted KS calculations, except for RPA and RPA+X as explained in the text. All values are in eV.

| $R$ (bohr) | 1.4 | 3 | 5 | 10 |
|---|---|---|---|---|
| EXX | −3.62 | −0.47 | −0.02 | 0.00 |
| PBE GGA | −4.53 | −1.27 | −0.03 | 0.00 |
| PBE0 hybrid | −4.52 | −1.07 | −0.03 | 0.00 |
| RPA | −4.73 | −1.44 | +0.54 | +0.20 |
| RPA+X | −4.86 | −1.45 | +0.34 | −0.25 |
| exact[a] | −4.75 | −1.56 | −0.10 | 0.00 |

[a]Reference [35].

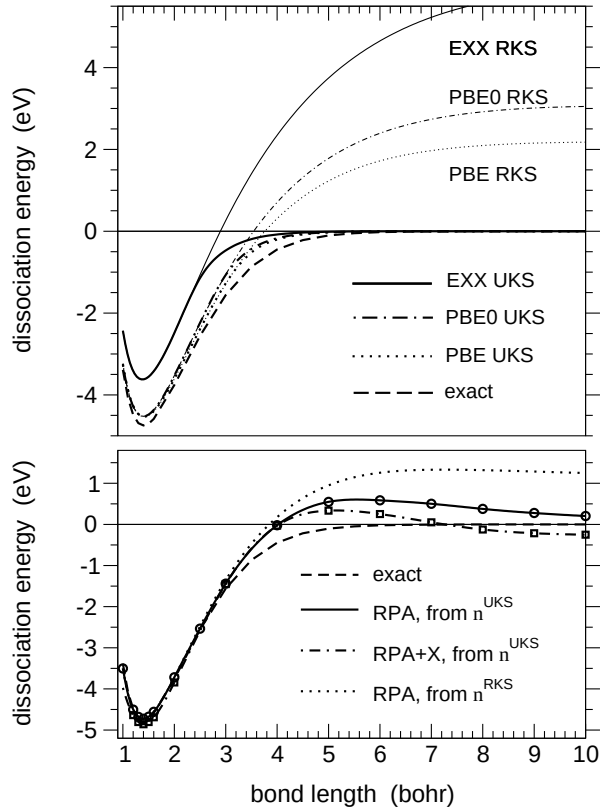


FIG. 5: Dissociation energy curve of $H_2$. The upper panel compares results for EXX, the PBE GGA, and the PBE0 hybrid functionals calculated in the self-consistent restricted (RKS) and unrestricted (UKS) KS formalism, with exact data from Ref. [35]. The lower panel compares the RPA and RPA+X curves, calculated with total densities $n^{\rm UKS}$ obtained from unrestricted EXX KS calculations, with exact data. Also shown is the RPA curve calculated with densities $n^{\rm RKS}$ from restricted EXX KS calculations.

RPA calculation using only the HOMO and LUMO EXX-KS states. As shown in the Appendix, this model RPA calculation yields the exact correlation (and total) energy for $R \to \infty$, and produces precisely the exact adiabatic connection of Fig. 2. Including the higher lying KS states, the RPA builds up spurious self-correlation in both the H atoms and the $H_2$ super-molecule, which however cancels out in the dissociation energy. This cancellation is indeed also reflected in the (identical) estimates of the local-density corrections (RPA+) in the atom and in the infinitely stretched molecule.

Figure 5 also demonstrates that for proper dissociation it is crucial to work with qualitatively correct densities, i.e., to start from a KS potential that takes into account the essential left-right correlation. Describing the system by the restricted KS formalism using the EXX, PBE GGA or PBE0 hybrid functionals leads to much too high total energies for the dissociating bond because the self-consistent EXX density is *qualitatively* wrong as explained in Sec. II. While the PBE GGA and PBE0 include correlation, improving over EXX, it is obvious from Fig. 5 that only the unrestricted KS formalism leads to reasonably accurate dissociation energies for larger $R$. The fact that the PBE0 curve raises too quickly above the true curve indicates that the error cancellation between exchange and correlation is significantly incomplete, as explained in Sec. III A. For $H_2$, PBE GGA clearly works better, and the lower energy solution appears only beyond $R \approx 4$ bohr, i.e. for a markedly larger bond length than in both the EXX and the PBE0 hybrid. In Table III we list the dissociation energies for the different functionals at various bond lengths.

The RPA curve is accurate around the $H_2$ equilibrium bond length and approaches the dissociation limit for large $R$. The success of the RPA lies in the fact that it does so (properly) as a functional of a singlet density only, rather than spin densities as in the traditional approximations for XC. Of course the density must ultimately come from a self-consistent KS calculation and potential, whereas we have approximated it non-selfconsistently. Our findings confirm that proper densities require accurate approximations also for the XC potential (the functional derivative of $E_{\rm XC}[n]$), as argued recently by Baerends [34]. In agreement with Ref. [34], our results also show that unoccupied KS states (and in particular the LUMO state) must be included in $E_{\rm XC}[n]$ in order to attain the correct dissociation limit.

An obvious shortcoming of the RPA compared to the unrestricted PBE GGA and PBE0 schemes is that its dissociation curve displays an unphysical bump for intermediate $R$ as seen in Fig. 5 and Tab. III. A similar behavior has been found for $N_2$ [25] and $Be_2$ [26, 76]. We believe that these deficiencies stem from the RPA itself, rather than our lack of self-consistency. In particular we have obtained essentially the same curves when we used densities derived from unrestricted LDA and GGA calculations. A more conclusive answer must either start from more accurate densities or await self-consistent calculations. Using an ansatz for the XC energy functional in terms of natural orbitals in a (approximately self-consistent) *singlet* KS calculation, Baerends and coworkers [32, 34] recently reported a dissociation curve of $H_2$ in very good agreement with the true curve for all $R$. The fact that for intermediate $R$ their curve is distinctly more accurate than our non-self-consistent RPA result clearly calls for further analysis of both approaches, including possible error cancellation between different components of the total energy. This is beyond the scope of our present study.

## V. EXTENSIONS BEYOND THE RPA

So far we have shown that the RPA gives a qualitatively correct account of the (differential) adiabatic connection of $H_2$, in contrast to semilocal or hybrid functionals, but needs to be improved for moderately large bond lengths. We now discuss possible extensions of the RPA as an ACFDT XC functional.

A known deficiency of the RPA is the spurious self-correlation in the absolute correlation energies, for the H atom as well as the $H_2$ molecule. For the one-electron H atom, self-correlation is eliminated by including the exact exchange kernel ($f_{\rm x}^{\lambda} = -\lambda v_{\rm ee}$) in the screening of the electronic Coulomb interaction, Eq. 2. For the two-electron $H_2$ the exact exchange kernel ($f_{\rm x}^{\lambda} = -\frac{\lambda}{2} v_{\rm ee}$ [46]), eliminates self-correlation to second order in $\lambda$ yet not to higher order. Using this RPA+X functional we obtain the dissociation energy of $H_2$ ($R = 1.4$ bohr) as $-4.86$ eV, about 0.1 eV below the true and our RPA values. Having estimated our computational accuracy at the same order, we feel cautious about the significance of the RPA+X result. On the other hand we find that the dissociation energy curve beyond the Coulson-Fisher point is not at all improved. To the contrary, while the RPA+X curve follows the RPA curve up to $\approx 4$ bohr, it drops below zero and approaches a negative constant for larger $R$. We regard this as a size-consistency problem in that the self-correlation error is eliminated in the H atoms, but reappears in the far stretched $H_2$. This is further corroborated in Appendix B. Our finding clearly suggests that in addition to exchange also correlation contributions need to be included in the XC kernel. A ready way to do so would be to employ the well-known adiabatic LDA kernel [77] or an energy-optimized adiabatic XC kernel [30].

As mentioned in Sec. II C the incorrect RPA short-ranged correlation, including self-correlation, may be corrected through a specially designed (semi-)local-density functional (RPA+). Although this improves upon the too negative RPA correlation energies as shown in Ref. [26], it again does not correct the deficiencies we observe in the RPA dissociation energy curve of $H_2$.

The limitation of RPA, as in any adiabatic treatment of the interacting linear response, might be that it treats only single excitations [78] and thus cannot take into account contributions to density fluctuations that correspond to doubly excited determinants and eventually also contribute to the correlation energy. As is well known, doubly excited determinants have larger weights in the asymptotic *interacting* wavefunctions of $H_2$ for both ground and excited states. For $R \to \infty$ this is evident from the corresponding exact Heitler-London wavefunctions (see e.g. Refs. [79] and [80]; for instance, the lowest $1\Sigma_g^+$ and $1\Sigma_u^+$ singlets are the symmetric and antisymmetric linear combinations, respectively, of the determinants $|\sigma_g\overline{\sigma}_g|$ and $|\sigma_u\overline{\sigma}_u|$ made up of the HOMO and LUMO). Double excitations imply additional poles in the (real frequency) interacting response and thus a strongly frequency-dependent XC kernel. Any such pole contributes to the spectral decomposition of the pair-correlation function or XC hole. While there is limited progress concerning the calculation of the excitation energies for certain doubly excited states within TDDFT [81], further analysis (and development) of the spatial and frequency dependence of such XC kernels is needed for applications in ACDFT XC functionals.

## VI. SUMMARY

The central message of this paper is that the Random Phase Approximation (RPA) resolves the long-standing symmetry dilemma encountered in *approximate* density functional theory when breaking the $H_2$ electron pair bond. We showed that the RPA produces the correct dissociation limit from a proper singlet KS density, without the need for artifical symmetry-breaking as in unrestricted Kohn-Sham theory for traditional local- or generalized-gradient functionals and hybrid exchange-correlation (XC) functionals. By analyzing the adiabatic connection, we showed that the RPA captures correctly the strong static (left-right) correlation that arises when the pair bond breaks. Local and gradient-corrected functionals make serious errors here, and even hybrids, which mimic this effect at equilibrium bond lengths, cannot account for the extreme static correlation in the dissociation limit. As the RPA yields an orbital-dependent XC functional, our results demonstrate the importance of including unoccupied KS states, in particular the LUMO state. We also showed that it is crucial to work with an accurate density, which we have constructed approximately in this study, and that could be improved by applying the RPA self-consistently. We further found the RPA dissociation curve to agree well with exact data near the equilibrium bond length of $H_2$. When the bond is stretched, it tends to the correct limit, unlike all the common restricted Kohn-Sham approaches. Noting that the RPA still leads to an unphysical repulsion of the hydrogens for intermediate bond lengths, we adressed inherent limitations and possible extensions of the RPA. Seen as a first step to realize fully nonlocal XC functionals by the adiabatic-connection fluctuation-dissipation formalism, we believe that the RPA provides a sound basis for quantitative refinements. Our study highlights $H_2$ as a significant benchmark system for assessing future progress beyond the RPA.

### Acknowledgments

We thank Ulf von Barth and Michael Seidl for discussions, and Robert van Leeuwen for comments on the Appendix and kindly providing us with his data of Ref. [63]. X.G. thanks the FNRS (Belgium) for financial support. We acknowledge financial support from the Communauté Francaise de Belgique (through a subvention "Actions de Recherche Concertées"), the Belgian Federal State ("Poles d'attraction Interuniversitaires", Phase V), and the European Union (contracts HPRN-CT-2002-00317, "EXCITING" Research Training Network "First-principles approach to the calculation of optical properties of solids", and NMP4-CT-2004-500198, "NANOQUANTA" Network of Excellence "Nanoscale Quantum Simulations for Nanostructures and Advanced Materials" ). K.B. was supported by the National Sci-

ence Foundation under grant CHE-0355405. Some of this work (K.B.) was performed at the Centre for Research in Adaptive Nanosystems (CRANN) supported by the Science Foundation Ireland (Award 5AA/G20041).

## Appendix

In part A of this Appendix we describe our computational method for evaluating the RPA XC energy. In part B we corroborate that the RPA total energy of $H_2$ at asymptotically large bond distances from a *spin-restricted* Kohn-Sham groundstate (i) becomes indeed equivalent to the total energy of two free H atoms as calculated in a *spin-unrestricted* formalism, in contrast to the case of the RPA+X kernel, (ii) for sufficiently large separations $R$ includes the expected $-C_6^{\rm RPA}/R^6$ van der Waals attraction.

### A. Computational Method

We have implemented the RPA functional in a pseudopotential plane-wave framework [82], handling the response functions, Eqs. 1 and 2, in their reciprocal space representation. Gauss-Legendre quadrature rules are used for the $\lambda$ and $iu$ integrations. For our study of $H_2$ the $-1/r$ attraction is replaced by a highly accurate norm-conserving pseudopotential [83]. The latter yields practically the exact energy of the H atom and dissociation energies to within 0.1 mHa when compared to full-potential results, for LDA, GGA, or EXX calculations. We place the $H_2$ molecule in a fcc supercell of 21 bohr side length. For the initial KS calculation we use a plane-wave cutoff energy of 30 Ha, and 12 Ha for the response functions. In the KS response we include unoccupied states up to 2.5 Ha explicitly and treat the higher ones through a closure relation. For the frequency integration we employ 12 supports for $R < 2$ bohr and up to 54 for larger $R$, concomitant with the closing of the HOMO-LUMO gap. For the coupling strength integration we use 4 to 11 supports to capture the stronger curvature of $U_{\rm XC}^\lambda$ with increasing $R$. From convergence tests we estimate that our total and dissociation energies are converged to well within 0.1 eV. Indeed our value for the $H_2$ dissociation energy in RPA, $-4.73$ eV, is in excellent agreement with previous work [25, 26].

### B. RPA XC for $H_2$ at large bond lengths

In this section we show analytically that within the RPA $\lim_{R\to\infty} E_{\rm tot}(H_2) = 2E_{\rm tot}(H)$, i.e. that the total energies of the infinitely stretched, *spin-compensated* $H_2$ molecule and of two separate *spin-polarized* H atoms are identical. We also show that this does not hold for the exact exchange kernel (RPA+X approximation). We will examine the density response of the $H_2$ molecule using the particle-hole formulation (in a product basis of the KS states) of time-dependent DFT [78], which is equivalent to the matrix formalism used in Sec. II C but more convenient for formal analysis. We emphasize that our analysis holds for the RPA as an adiabatic approximation only, and does not address the effects of double excitations that require a non-adiabatic (frequency-dependent) correlation kernel as argued in Sec. V.

For the spin-compensated molecule the response function for some coupling strength $\lambda$ can be written as

$$\chi^\lambda[H_2](\mathbf{r},\mathbf{r}';\omega) = \sum_n Q_n^\lambda(\mathbf{r}) \frac{4\Omega_n(\lambda)}{\omega^2-\Omega_n^2(\lambda)} Q_n^{\lambda\,*}(\mathbf{r}') \quad , \quad (16)$$

where $\Omega_n(\lambda)$ are the transition frequencies and $Q_n^\lambda$ are the associated amplitudes. The $\Omega_n(\lambda)$ are the positive square roots of the eigenvalues of the matrix

$$M_{ij,kl}(\lambda) = \omega_{ij}^2\delta_{ik}\delta_{jl} + 4\sqrt{\omega_{ij}} f_{ij,kl}^{\rm HXC}(\lambda)\sqrt{\omega_{kl}} \quad (17)$$

involving all possible KS excitations from an occupied KS state $\phi_i$ to an unoccupied KS state $\phi_j$, with respective KS transition frequencies $\omega_{ij} = \epsilon_j - \epsilon_i$. Here $f_{ij,kl}^{\rm HXC}(\lambda) = \int d^3r d^3r' \phi_i(\mathbf{r})\phi_j^*(\mathbf{r}) f_{\rm HXC}^\lambda(\mathbf{r},\mathbf{r}')\phi_k^*(\mathbf{r}')\phi_l(\mathbf{r}')$ denotes the matrix elements of the Hartree and XC kernel, and it is assumed that one works in the adiabatic approximation, i.e. that the XC kernel is frequency independent. From the eigenvectors $U_{ij,n}^\lambda$ of $M_{ij,kl}(\lambda)$, one obtains the spectral components

$$Q_{ij,n}^\lambda = \sqrt{\omega_{ij}/\Omega_n(\lambda)}\ U_{ij,n}^\lambda \quad (18)$$

of the amplitudes $Q_n^\lambda(\mathbf{r}) = \sum_i^{\rm occ.}\sum_j^{\rm unocc.} Q_{ij,n}^\lambda \phi_i^*(\mathbf{r})\phi_j(\mathbf{r})$. In the RPA, $f_{\rm HXC}^\lambda = \lambda v_{\rm ee}$.

Consider now the $H_2$ molecule at large $R$. For any finite number $N$ of (bound) KS states, $R$ can be chosen large enough such that the molecular orbitals can be approximated by the bonding and antibonding linear combinations of the atomic orbitals $a_i(\mathbf{r})$ and $b_i(\mathbf{r})$ of the H atoms A and B respectively:

$$\phi_{i\pm}(\mathbf{r}) \simeq (2\mp 2S_i)^{-1/2}\{a_i(\mathbf{r}) \pm b_i(\mathbf{r})\} \quad , \quad (19)$$

where $S_i$ is the overlap integral. Similarly, we approximate the respective eigenenergies $E_{i\pm} \simeq \epsilon_i$ by the atomic eigenenergies $\epsilon_i$, except for the HOMO and LUMO energies $E_{0\pm}$ whose gap we write as $E_g = E_{0-} - E_{0+}$.

In the (imaginary frequency) KS response $\chi^0[H_2]$ of the molecule, we first split off the HOMO-LUMO transition which is well separated from the higher ones, and define:

$$\delta\chi^0[H_2](\mathbf{r},\mathbf{r}',iu) = -4E_g \frac{q(\mathbf{r})q(\mathbf{r}')}{u^2+E_g^2} \quad , \quad (20)$$

where $q(\mathbf{r}) = \phi_{0+}(\mathbf{r})\phi_{0-}(\mathbf{r}) = (2\sqrt{1-S_0^2})^{-1}(|a_0(\mathbf{r})|^2 - |b_0(\mathbf{r})|^2)$. For $R\to\infty$, the remainder $\tilde\chi^0[H_2] =: \chi^0[H_2] - \delta\chi^0[H_2]$ can readily be shown to split (up to exponentially

decreasing corrections) into atomic contributions $\chi^0[\mathrm{H_A}]$ and $\chi^0[\mathrm{H_B}]$, where:

$$\chi^0[\mathrm{H_A}](\mathbf{r},\mathbf{r}';iu) = -\sum_{j=1}^{N/2} 4(\epsilon_j-\epsilon_0)\frac{a_0^*(\mathbf{r})a_j(\mathbf{r})a_j^*(\mathbf{r}')a_0(\mathbf{r}')}{u^2+(\epsilon_j-\epsilon_0)^2} \quad , \tag{21}$$

with a similar definition for $\chi^0[\mathrm{H_B}]$. $\chi^0[\mathrm{H_A}]$ and $\chi^0[\mathrm{H_B}]$ are formally equivalent to the KS reponse of a free *spin-polarized* H atom (see however the discussion of RPA+X below). Hence we asymptotically get:

$$\chi^0[\mathrm{H_2}] = \chi^0[\mathrm{H_A}] + \chi^0[\mathrm{H_B}] + \delta\chi^0[\mathrm{H_2}] + \mathcal{O}(\exp.) \quad . \tag{22}$$

As for the asymptotic RPA response ($R\to\infty$), inspection of Eq. 17 shows that the lowest eigenvalue $\Omega_0^2(\lambda)$ (i.e. the singlet excitation energy) exponentially tends to zero and is well separated from the others. Indeed,

$$\Omega_0^2(\lambda) = E_g^2 + 4\lambda K_0 E_g + \lambda^2 P(\lambda) E_g + \mathcal{O}\left\{(\lambda E_g)^2\right\} \quad , \tag{23}$$

where the HOMO-LUMO exchange integral $K_0 = \langle\phi_{0-}\phi_{0+}|\hat{v}_{\mathrm{ee}}|\phi_{0+}\phi_{0-}\rangle \simeq U[\mathrm{H}] - (2R)^{-1} + \mathcal{O}(\exp.)$ reduces asymptotically to the atomic Hartree energy, and $P$ is an (here) unspecified, yet smooth function of $\lambda$. Note that the first two terms on the R.H.S. of Eq. 23 also follow from the single pole approximation to TDDFT excitation energies, and that the remainder describes corrections due to the coupling with higher KS excitations [84]. The corresponding eigenvector is $U^\lambda_{ij,0} = \delta_{ij,0+0-} + \mathcal{O}(\lambda\sqrt{E_g})$. Hence we can split the asymptotic RPA response of $H_2$ as follows:

$$\chi^\lambda[\mathrm{H_2}] = \tilde{\chi}^\lambda[\mathrm{H_2}] + \delta\chi^\lambda[\mathrm{H_2}] + \mathcal{O}(\exp.) \quad , \tag{24}$$

where

$$\delta\chi^\lambda[\mathrm{H_2}](\mathbf{r},\mathbf{r}';iu) = -4E_g\frac{q(\mathbf{r})q(\mathbf{r}')}{u^2+\Omega_0^2(\lambda)} \quad , \tag{25}$$

and $\tilde{\chi}^\lambda = (1-\tilde{\chi}^0\lambda v_{\mathrm{ee}})^{-1}\tilde{\chi}^0$ is the contribution from the other eigenvalues and eigenvectors of the matrix $M_{ij,kl}(\lambda)$. For large $R$, we can further write $\tilde{\chi}^\lambda$ as the sum of the RPA responses of the H atoms, $\chi^\lambda[\mathrm{H_{A,B}}]$, and an inter-atomic correction [6], $\Delta\chi^\lambda[\mathrm{H_2}]$:

$$\tilde{\chi}^\lambda[\mathrm{H_2}] = \chi^\lambda[\mathrm{H_A}] + \chi^\lambda[\mathrm{H_B}] + \Delta\chi^\lambda[\mathrm{H_2}] \quad . \tag{26}$$

The atomic part

$$\chi^\lambda[\mathrm{H}] = (1-\chi^0[\mathrm{H}]\lambda v_{\mathrm{ee}})^{-1}\chi^0[\mathrm{H}] \tag{27}$$

is formally equivalent to the RPA response of a *spin-polarized* H atom.

Using the response functions as decomposed in Eqs. 22, 24 and 26, the RPA correlation energy for stretched $H_2$ reads

$$E_{\mathrm{c}}^{\mathrm{RPA}}[\mathrm{H_2}] = -\int_0^1 d\lambda \int_0^\infty \tfrac{du}{2\pi}\,\mathrm{Tr}[v_{\mathrm{ee}}\{\chi^\lambda[\mathrm{H_2}](iu) - \chi^0[\mathrm{H_2}](iu)\}] \tag{28}$$

$$= E_{\mathrm{c}}^{\mathrm{RPA}}[\mathrm{H_A}] + E_{\mathrm{c}}^{\mathrm{RPA}}[\mathrm{H_B}] + \Delta E_{\mathrm{c}}^{\mathrm{RPA}}[\mathrm{H_2}] + \delta E_{\mathrm{c}}^{\mathrm{RPA}}[\mathrm{H_2}] \quad . \tag{29}$$

Here $E_{\mathrm{c}}^{\mathrm{RPA}}[\mathrm{H}]$ is the RPA correlation energy of a *spin-polarized* H atom (associated with $\chi^\lambda[\mathrm{H}] - \chi^0[\mathrm{H}]$), $\Delta E_{\mathrm{c}}^{\mathrm{RPA}}[\mathrm{H_2}]$ comes from $\Delta\chi^\lambda[\mathrm{H_2}]$, and $\delta E_{\mathrm{c}}^{\mathrm{RPA}}[\mathrm{H_2}]$ from $\delta\chi^\lambda[\mathrm{H_2}] - \delta\chi^0[\mathrm{H_2}]$. Expanding $\Delta\chi^\lambda[\mathrm{H_2}]$ in $\lambda v_{\mathrm{ee}}$ one can show, analogously to the case of interacting closed-shell systems [6], that the leading, second-order contribution to $\Delta E_{\mathrm{C}}^{\mathrm{RPA}}[\mathrm{H_2}]$ recovers the van der Waals interaction between the H atoms, i.e.

$$\Delta E_{\mathrm{C}}^{\mathrm{RPA}}[\mathrm{H_2}] \simeq -C_6^{\mathrm{RPA}}[\mathrm{H}]R^{-6} \quad , \tag{30}$$

with the atomic $C_6$ coefficient obtained within the RPA. We next consider the HOMO-LUMO part of the response, writing $\delta E_{\mathrm{c}}^{\mathrm{RPA}}[\mathrm{H_2}] = \int_0^1 d\lambda\, \delta U_{\mathrm{C}}^{\mathrm{RPA}}[\mathrm{H_2}](\lambda)$, where

$$\begin{aligned}\delta U_{\mathrm{C}}^{\mathrm{RPA}}[\mathrm{H_2}](\lambda) &= -\int_0^\infty \tfrac{du}{2\pi}\,\mathrm{Tr}[v_{\mathrm{ee}}\{\delta\chi^\lambda(iu) - \delta\chi^0(iu)\}] \\ &= K_0\left(\tfrac{E_g}{\Omega_0(\lambda)} - 1\right) \\ &= K_0\left(\left\{1 + 4\lambda\tfrac{K_0}{E_g} + \tfrac{\lambda^2 P(\lambda)}{E_g} + \mathcal{O}(\lambda^2)\right\}^{-1/2} - 1\right) \quad .\end{aligned} \tag{31}$$

The integration over $\lambda$ then yields asymptotically:

$$\delta E_{\mathrm{C}}^{\mathrm{RPA}}[\mathrm{H_2}] = -K_0 + \mathcal{O}(\sqrt{K_0 E_g}) \tag{32}$$

$$\simeq -U[\mathrm{H}] + (2R)^{-1} + \mathcal{O}(\exp.) \quad . \tag{33}$$

The term $\delta E_{\mathrm{c}}^{\mathrm{RPA}}$ is associated with the static correlation

due to the (nearly) degenerate HOMO and LUMO KS states. Adding $E_{\rm x}[{\rm H}_2] \sim 2E_{\rm x}[{\rm H}] + U[{\rm H}] - (2R)^{-1} + \mathcal{O}(\text{exp.})$ to $E_{\rm C}^{\rm RPA}[{\rm H}_2]$ we last get for the RPA XC energy

$$E_{\rm XC}^{\rm RPA}[{\rm H}_2] \simeq 2E_{\rm XC}^{\rm RPA}[{\rm H}] - C_6^{\rm RPA} R^{-6} \quad . \qquad (34)$$

The kinetic, electron-nucleus, nucleus-nucleus and Hartree components of the total energy of $H_2$ are easily shown to also approach those of the free atoms for $R \to \infty$. Hence the RPA obeys the expected result $\lim_{R\to\infty} E_{\rm tot}^{\rm RPA}[{\rm H}_2] = 2E_{\rm tot}^{\rm RPA}[{\rm H}]$.

Several remarks are in order:

*Leading R-dependence of $E_{\rm C}^{RPA}[H_2]$ for $R \to \infty$:* Equation 34 states that the $C_6^{\rm RPA} R^{-6}$ van der Waals term is the leading correction to the asymtpotic RPA XC energy. This finding rests on the result of Eq. 33 that the static correlation term $\delta E_{\rm C}^{\rm RPA}[{\rm H}_2]$ follows the $(2R)^{-1}$ behavior of $K_0(R)$, i.e. that it contains no multipole terms of higher power than $R^{-1}$ up to $R^{-6}$. The latter holds if (i) the HOMO and LUMO are represented by linear combinations of $s$-like atomic functions, as is appropriate for large $R$ and as we had assumed. Then higher order terms in $K_0(R)$ decay in fact exponentially with $R$, as can be seen from a multipole decomposition of $K_0$. A further condition is that (ii) the HOMO-LUMO gap (and thus $\sqrt{K_0 E_g}$ in Eq. 32) decays exponentially, as is expected for Kohn-Sham states (as opposed to a Hartree-Fock calculation, where $E_g \propto R^{-1}$) and which we have verified numerically in the range $R = 4 \ldots 10$ bohr. Of course, for the bond lengths considered here the van der Waals term is in fact marginal: for instance, $C_6^{\rm RPA} R^{-6} \sim 8$ meV and $\sim 0.1$ meV at $R = 5$ and 10 bohr, respectively, i.e. more than an order of magnitude smaller than the total RPA errors given in Tab. III (using $C_6^{\rm RPA} \sim 4.6$ a.u., calculated from the atomic dipole polarizability). Clearly, the RPA dissociation energy curve is still dominated in the range $R = 4 \ldots 10$ bohr by the static correlation term of Eqs. 32 and 33, as we further discuss in the next paragraph.

*Repulsion at intermediate R and role of self-consistency:* From Eq. 31 we can interpret the ratio $\alpha^{\rm RPA}(\lambda) = K_0 E_g / \Omega_0^{\rm RPA}(\lambda) < K_0$ as a correction to the exact asymptotic adiabatic connection (Fig. 2) that decays exponentially with $R \to \infty$, turning on static correlation. $\alpha^{\rm RPA}(\lambda)$ yields a positive $\mathcal{O}(\sqrt{K_0 E_g})$ contribution to the RPA exchange-correlation energy (see Eq. 33). While this contribution is expected to die out exponentially like $E_g$, it may still be significant around $R = 10$ bohr, showing up as a spuriously repulsive dissociation curve. Our $E_g \sim 10^{-2}$ eV at $R = 10$ bohr is indeed compatible with the $\sim 0.2$ eV error we find from our RPA calculation at this bond length (this estimate follows from the single transition model discussed at the end of this appendix). We cannot rule out that in a self-consistent treatment $E_g$ decays (sufficiently) more rapidly compared to our present non-selfconsistent calculation.

*Behavior of $E_{\rm C}^{RPA+X}[H_2]$ for $R \to \infty$:* For the exact exchange kernel [46] the same analysis of the molecular correlation energy as for the RPA can be carried through with $\lambda$ replaced by $\lambda/2$. For $R \to \infty$, the static correlation term $\delta E_{\rm C}^{\rm RPA+X}[{\rm H}_2] \sim -U[{\rm H}] + (2R)^{-1} + \mathcal{O}(\text{exp.})$ remains the same as in the RPA. However the atomic terms in Eq. 29 do not vanish, in contrast to the RPA+X correlation energy of *spin-polarized* free H atoms. Indeed, for a free H atom the spin-density responses $\chi_{\sigma\sigma'}^{\lambda\,\rm RPA+X}[{\rm H}]$ and $\chi_{\sigma\sigma'}^{0}[{\rm H}]$ are identical, as is easily seen from the spin-resolved Dyson equation (see e.g. Ref. [77]). Thus $E_{\rm C}^{\rm RPA+X}[{\rm H}] = 0$ and $E_{\rm tot}^{\rm RPA+X}[{\rm H}] = -0.5$ a.u. However, in the spin-compensated stretched $H_2$ both the spin-up and the spin-down (noninteracting) KS electrons are found with a 50% chance on either nucleus. Thus what enters as the atomic term $\chi^0[{\rm H}]$ in Eqs. 22 and 27 corresponds in fact to the KS spin-response of a fictitious spin-compensated H atom (denoted H') with half occupied $1s\uparrow$ and $1s\downarrow$ states. The corresponding RPA+X correlation energy appearing on the R.H.S. of Eq. 29 is therefore $E_{\rm C}^{\rm RPA+X}[{\rm H'}] \simeq E_{\rm C}^{\rm RPA}[{\rm H}]/2$ (estimated to second order in $\lambda v_{\rm ee}$). Consequently, $\lim_{R\to\infty}(E_{\rm tot}^{\rm RPA+X}[{\rm H}_2] - E_{\rm tot}^{\rm RPA+X}[{\rm H}]) \simeq E_{\rm C}^{\rm RPA}[{\rm H}] < 0$. In an actual calculation we indeed find that the RPA+X potential energy curve drops below zero beyond $R \simeq 7$ bohr (see Fig. 5).

The RPA yields $E_{\rm C}^{\rm RPA}[{\rm H'}] = E_{\rm C}^{\rm RPA}[{\rm H}]$, i.e. the distinction between H' and H does not matter. This (spurious) RPA self-correlation energy ($E_c^{\rm RPA}[{\rm H}] \approx -23$ mHa per atom, using the exact $n_{\rm H}$) appears for the free atoms and the stretched $H_2$ and thus cancels out. In a spin-polarized one-electron system, the exchange kernel fully cancels the Coulomb kernel, leading to $E_{\rm C}^{\rm RPA+X}[{\rm H}] = 0$. In a spin-compensated two-electron system like $H_2$, correlation should arise only from the interaction of opposite-spin electrons. For the RPA+X kernel it is easy to see that there is zero like-spin correlation up to second order in $\lambda v_{\rm ee}$ (although non-zero in higher orders). The fact that the dynamical correlation associated with $\tilde{\chi}^\lambda$ does not vanish for the RPA+X kernel in the infinitely stretched $H_2$ may then be seen as a failure to suppress opposite-spin correlation between the electrons on either atomic site.

Had we treated the stretched $H_2$ in a spin-polarized KS scheme, the two electrons would be localized with opposite spin on either nucleus right from the beginning. While we have not performed this calculation, we expect from our above discussion that both the RPA and RPA+X yield $\lim_{R\to\infty} E_{\rm tot}[{\rm H}_2] = 2E_{\rm tot}[{\rm H}]$ in this case.

*Model based on the HOMO-LUMO transition only:* If we include in the response only the HOMO and LUMO KS states, we get a "minimal", two-state model of $H_2$ in which all effects of higher transitions are ignored. Then $E_{\rm C}[{\rm H}_2]$ in Eq. 29 is given by just the static correlation term $\delta E_{\rm C}[{\rm H}_2]$:

$$\begin{aligned} E_{\rm C}[{\rm H}_2] &\sim \tfrac{E_g}{\kappa}\left(\sqrt{1+\tfrac{2\kappa K_0}{E_g}} - 1\right) - K_0 \\ &\simeq -K_0 + \sqrt{2K_0 E_g/\kappa} \quad , \quad \text{for } R \to \infty \quad , \end{aligned} \qquad (35)$$

for the RPA ($\kappa = 2$) as well as the RPA+X ($\kappa = 1$). The asymptotic $R$-dependence of this minimal $E_{\rm C}[{\rm H}_2]$ is

again that given by Eq. 33. Hence within the minimal model also the RPA+X, like the RPA, correctly yields the total energy of the dissociated $H_2$ as that of two free H atoms. Indeed, inspection of Eq. 31 shows that both RPA and RPA+X recover the exact adiabatic connection for $R \to \infty$, i.e. that $\delta U_c(\lambda > 0) = -U[\mathrm{H}]$. Note however that due to the closing HOMO-LUMO gap for $R \to \infty$ the initial slope $dU_c^{\mathrm{RPA+X}}(\lambda)/d\lambda|_{\lambda=0} = -K_0^2/E_g$ eventually diverges, as does the the GL2 correlation energy. Independently of our work, an analogous minimal model has been recently obtained by van Leeuwen and coworkers, studying total energy functionals based on Green functions [85].


[1] P. Hohenberg and W. Kohn, Phys. Rev. **136**, B864 (1964).
[2] W. Kohn and L.J. Sham, Phys. Rev. **140**, A1133 (1965).
[3] W. Koch and M.C. Holthausen, *A Chemist's Guide to Density Functional Theory* (Wiley-VCH, Weinheim, 2001).
[4] A.D. Becke, J. Chem. Phys. **98**, 5648 (1993); *ibid.* **104**, 1040 (1996).
[5] J.P. Perdew, M. Ernzerhof, and K. Burke, J. Chem. Phys. **105**, 9982 (1996).
[6] J. Dobson, in "Topics of Condensed Matter Physics", edited by M.P. Das (Nova, New York 1994), p. 121; see also `cond-mat/0311371`.
[7] J.F. Dobson and B.P. Dinte, Phys. Rev. Lett. **76**, 1780 (1996).
[8] W. Kohn, Y. Meir, and D.E. Makarov, Phys. Rev. Lett. **80**, 4153 (1998).
[9] E. Engel, A. Höck, and R.M. Dreizler, Phys. Rev. A **61**, 032502 (2000).
[10] P. García-Gonzáles and R.W. Godby, Phys. Rev. Lett. **88**, 056406 (2002).
[11] M. Ernzerhof, K. Burke, and J.P. Perdew, in: *Recent Developments in Density Functional Theory*, edited by J.M. Seminario (Elsevier, Amsterdam, 1997).
[12] T. Bally and G. Nahsari Sastry, J. Phys. Chem. A **101**, 7923 (1997).
[13] M. Sodupe, J. Bertran, L. Rodríguez-Santiago, and E.J. Baerends, J. Phys. Chem. A **103**, 166 (1999).
[14] M. Ernzerhof, J.P. Perdew, and K. Burke, in: *Topics in Current Chemistry*, Vol. 180, edited by R.F. Nalewajski (Springer, Berlin, 1996), p. 1.
[15] O.V. Gritsenko, P.R.T. Schipper, and E.J. Baerends, J. Chem. Phys. **107**, 5007 (1997).
[16] J.P. Perdew, A. Savin, and K. Burke, Phys. Rev. A **51**, 4531 (1995).
[17] A.M. Lee and N.C. Handy, J. Chem. Soc. Faraday Trans. **89**, 3999 (1993).
[18] C.D. Sherill, M.S. Lee, and M. Head-Gordon, Chem. Phys. Lett. **302**, 425 (1999).
[19] M. Filatov and S. Shaik, Chem. Phys. Lett. **332**, 409 (2000); J. Phys. Chem. A **104**, 6628 (2000).
[20] R. Pollet, A. Savin, T. Leininger, and H. Stoll, J. Chem. Phys. **116**, 1250 (2002).
[21] D.C. Langreth and J.P. Perdew, Solid State Commun. **17**, 1425 (1975); Phys. Rev. B **15**, 2884 (1977).
[22] J.P. Perdew and K. Schmidt, in: *Density Functional Theory and Its Application to Materials*, edited by V. Van Doren, C. Van Alsenoy, and P. Geerlings, (AIP, Melville, New York, 2001).
[23] S. Kurth and J.P. Perdew, Phys. Rev. B **59**, 10461 (1999).
[24] J.F. Dobson and J. Wang, Phys. Rev. Lett. **82**, 2123 (1999).
[25] F. Furche, Phys. Rev. B **64**, 195120 (2001).
[26] M. Fuchs and X. Gonze, Phys. Rev. B **65**, 235109 (2002).
[27] H. Rydberg *et al.*, Phys. Rev. Lett. **91**, 126402 (2003).
[28] M. Dion, H. Rydberg, E. Schröder, D.C. Langreth, and B.I. Lundqvist, Phys. Rev. Lett. **92**, 246401 (2004).
[29] Z. Yan, J.P. Perdew, and S. Kurth, Phys. Rev. B **61**, 16430 (2000).
[30] J.F. Dobson and J. Wang, Phys. Rev. B **62**, 10038 (2000).
[31] J.F. Dobson, J. Wang, and T. Gould, Phys. Rev. B **66**, 081108 (2002).
[32] M. Grüning, O.V. Gritsenko, and E.J. Baerends, J. Chem. Phys. **118**, 7183 (2003).
[33] J.M. Herbert and J.E. Harriman, Chem. Phys. Lett. **382**, 142 (2003).
[34] E.J. Baerends, Phys. Rev. Lett. **87**, 133004 (2001).
[35] W. Kolos and C.C. Roothaan, Rev. Mod. Phys. **32**, 219 (1960).
[36] Of course, one never works with this decomposition within DFT. The interpretation in terms of covalent and ionic parts is however quite natural when $\Psi^{\mathrm{KS}}$ is analyzed as a many-electron wavefunction.
[37] C.A. Coulson and I. Fisher, Phil. Mag. **40**, 386 (1949).
[38] O. Gunnarsson and B. Lundqvist, Phys. Rev. B **13**, 4274 (1976).
[39] R. van Leeuwen, O.V. Gritsenko, and E.J. Baerends in: *Topics in Current Chemistry*, Vol. 180, edited by R.F. Nalewajski (Springer, Berlin, 1996), p. 107.
[40] C. Filippi, S.B. Healy, P. Kratzer, E. Pehlke, and M. Scheffler, Phys. Rev. Lett. **89**, 166102 (2002).
[41] R. Bauernschmitt and R. Ahlrichs, J. Chem. Phys. **104**, 9047 (1996).
[42] J. Gräfenstein, E. Kraka, and D. Cremer, Chem. Phys. Lett. **288**, 593 (1998).
[43] S. Grimme and M. Waletzke, J. Chem. Phys. **111**, 5645 (1999).
[44] P.R.T. Schipper, O.V. Gritsenko, and E.J. Baerends, J. Chem. Phys. **111**, 4056 (1999).
[45] A. Görling and M. Levy, Phys. Rev. A **50**, 196 (1994); for a review see also: T. Grabo, T. Kreibich, S. Kurth, and E.K.U. Gross, in: *Strong Coulomb Correlations in Electronic Structure: Beyond the LDA*, edited by V.I. Anisimov (Gordon and Breach, 1999), p. 203.
[46] M. Petersilka, U.J. Gossmann, and E.K.U. Gross, Phys. Rev. Lett. **76**, 1212 (1996).
[47] A. Görling and M. Levy, Phys. Rev. B **47**, 13105 (1993).
[48] A.D. Becke, J. Chem. Phys. **109**, 2092 (1998).
[49] T. Van Voorhis and G.E. Scuseria, J. Chem. Phys. **109**, 400 (1998).
[50] J. Tao, J.P. Perdew, V.N. Staroverov, and G.E. Scuseria Phys. Rev. Lett. **91**, 146401 (2003).
[51] C.-O. Almbladh, U. von Barth, and R. van Leeuwen, Int.

J. Mod. Phys. B **13**, 535 (1999).
[52] N.E. Dahlen and U. von Barth, J. Chem. Phys. **120**, 6826 (2004).
[53] L.J. Holleboom and J.G. Snijders, J. Chem. Phys. **93**, 5826 (1990).
[54] F. Aryasetiawan, T. Miyake, and K. Terakura, Phys. Rev. Lett. **88**, 166401 (2002); *ibid.* **90**, 189702 (2003).
[55] M. Fuchs, K. Burke, Y.-M. Niquet, and X. Gonze, Phys. Rev. Lett. **90**, 189701 (2003).
[56] Y.-M. Niquet, M. Fuchs, and X. Gonze, J. Chem. Phys. **118**, 9504 (2003).
[57] Y.-M. Niquet, M. Fuchs, and X. Gonze, Phys. Rev. A **68**, 032507 (2003).
[58] J.P. Perdew and Y. Wang, Phys. Rev. B **45**, 13244 (1992).
[59] J.P. Perdew, K. Burke, and M. Ernzerhof, Phys. Rev. Lett. **77**, 3685 (1996).
[60] M. Levy and J.P. Perdew, Phys. Rev. A **32**, 2010 (1985).
[61] M. Ernzerhof, Chem. Phys. Lett. **263**, 499 (1996).
[62] K. Burke, M. Ernzerhof, and J.P. Perdew, Chem. Phys. Lett. **265**, 115 (1997).
[63] R. van Leeuwen, Ph.D. thesis, Vrije Universiteit, Amsterdam (1996).
[64] O.V. Gritensko and E.J. Baerends, Phys. Rev. A **54**, 1957 (1996).
[65] We interpolate the (unknown) exact curve in $\lambda \in [0,1]$ by $\Delta U_{\rm XC}(\lambda) = \Delta E_{\rm X} + \frac{\Delta U'_{\rm XC}(0)\lambda p(\lambda)}{1+\alpha\lambda p(\lambda)}$ where $\alpha = \frac{\Delta U'_{\rm XC}(0)}{\Delta U_{\rm C}} - \frac{1}{p(1)}$. Our interpolation reproduces $\Delta E_{\rm X}$, $\Delta U'_{\rm XC}(0)$, and $\Delta U_{\rm XC}$ as given in Tabs. I and II. For $R = 1.4$ bohr it integrates to $\Delta E_{\rm XC} = -2.07$ eV, where we have set $p(\lambda) \equiv 1$. For $R = 5$ bohr we have chosen $p(\lambda) = 1 + \beta\lambda e^{-\gamma\lambda}$, adjusting $\beta$ and $\gamma$ to yield $\Delta E_{\rm XC} = 0.82$ eV and also the strong interaction limit of $U_{\rm XC}[{\rm H}_2](\lambda)$ [M. Seidl, private communication].
[66] A. Puzder, M.Y. Chou, and R.Q. Hood, Phys. Rev. A **64**, 022501 (2001).
[67] A. Savin, F. Colonna, and M. Allavena, J. Chem. Phys. **115**, 6827 (2001).
[68] F. Colonna, D. Maynau, and A. Savin, Phys. Rev. A **68**, 012505 (2003).
[69] R.Q. Hood, M.Y. Chou, A.J. Williamson, G. Rajagopal, and R.J. Needs, Phys. Rev. B **57**, 8972 (1998).
[70] R.J. Magyar, W. Terilla, and K. Burke, J. Chem. Phys. **119**, 696 (2003).
[71] M. Seidl, J.P. Perdew, and S. Kurth, Phys. Rev. Lett. **84**, 5070 (2000).
[72] M. Fuchs and X. Gonze, unpublished.
[73] C. Adamo and V. Barone, J. Chem. Phys. **110**, 6158 (1999).
[74] E. Clementi and S.J. Chakravorty, J. Chem. Phys. **93**, 2591 (1990).
[75] C.J. Umrigar and X. Gonze, Phys. Rev. A **50**, 3827 (1994).
[76] M. Fuchs and X. Gonze, unpublished.
[77] M. Lein, E.K.U. Gross, and J.P. Perdew, Phys. Rev. B **61**, 13431 (2000).
[78] M.E. Casida, in *Recent Developments and Applications in Density Functional Theory*, edited by J.M. Seminario (Elsevier, Amsterdam 1996).
[79] J.C. Slater, Quantum Theory of Molecules and Solids, Vol. 1 (McGraw-Hill, New York, 1963), p. 60.
[80] O.V. Gritsenko, S.J.A. van Gisbergen, A. Görling, and E.J. Baerends, J. Chem. Phys. **113**, 8478 (2000).
[81] N.T. Maitra, F. Zhang, R.J. Cave, and K. Burke, J. Chem. Phys. **120**, 5932 (2004).
[82] X. Gonze *et al.*, Comput. Materials Science **25**, 478 (2002).
[83] M. Fuchs and M. Scheffler, Comput. Phys. Commun. **107**, 67 (1999).
[84] H. Appel, E.K.U. Gross, and K. Burke, Phys. Rev. Lett. **90**, 043005 (2003).
[85] R. van Leeuwen, private communication.